Particle Sampling by TEM Grid Filtration

Badr R'Mili, Olivier Le Bihan, Christophe Dutouquet, Olivier Aguerre-Chariol, Emeric Frejafon

Particle Sampling by TEM Grid Filtration

B. R'mili, O.L.C. Le Bihan, C. Dutouquet, O. Aguerre-Charriol, E. Frejafon.

Address correspondence to Olivier Le Bihan, F60550 Verneuil en Halatte.

E-mail: Olivier.le-bihan@ineris.fr

ABSTRACT

Transmission electron microscopy (TEM) coupled with energy dispersive X-ray (EDX) offers a very comprehensive tool for individual particle analysis allowing the determination of size, morphology, specific surface, and elemental composition. This information is needed in aerosol studies, especially in the field of nanomaterials. However, observations with TEM require a controlled sampling on an adapted analysis support, namely TEM grid. Techniques allowing sampling on TEM grids are of great interest to aerosol analysis. Indeed, sample preparation is not required, thereby gaining time and avoiding a risk for the sample to be altered.

The present study evaluates the efficiency of a new particle collection technique based on filtration through one class of TEM dedicated supports, namely TEM porous grids.

Two types of porous grids, considered as the best on the market for this application, have been put to the test: the "Quantifoil" type porous grid which has a regular structure, and the "Holey" type (Agar Scientific). A filter holder has been developed specifically for this application, the MPS® ("Mini-Particle Sampler"®).

Experimental tests have been carried out with a flow rate of 0.3 l.min^{-1}. They show that the collection is operational in the 5 nm – 150 nm size range with a minimum efficiency of 15-18% around 30 nm. Simulation confirms these results and shows an increased efficiency even below 5 nm and beyond 150 nm.

The filter holder MPS® designed in this study is a low cost, portable versatile and easy to use tool.

APPENDIX

Variable	Description		Variable	Description
A_0	area occupied by the opening of a beam hole R_0		$N_{stage\ 2}$	Number concentration dowstream the holder during stage 2 (#.cm^{-3})
C_c	Cunningham slip factor		P	Porosity of the membrane
D	Coefficient of Brownian diffusion		Pe_p	Peclet number related to a pore diameter
D_0	pore diameter (cm)		P_t	Penetration
d_p	particle diameter (cm)		Q	Sampling flow (l/min)
E	efficiency of collection		R	Interception parameter
E_D	deposition efficiency due to diffusion		Re	Reynold's number
E_{Im}	deposition efficiency due to impaction		R_e	External radius of the unit hole (cm)
E_{In}	deposition efficiency due to interception		R_0	pore radius (cm)
Kn	Knudsen's number		r_p	particle radius (cm)
m	particle mass (g)		S	Section of filter holder upstream of the TEM grid (cm^2)
N_{Dw}	Number concentration downstream a filter (#.cm^{-3})		U_0	frontal velocity (opposite membrane) fluid flow (cm/s)
N_o	Number of holes by unit of surface		ρ_P	particle density (g/cm^3)
N_{Up}	Number concentration upstream a filter (#.cm^{-3})		η	fluid viscosity (Pa.s)
$N_{stage\ 1}$	Number concentration downstream the holder during stage 1 (#.cm^{-3})		λ_g	Free mean flow of gas molecules
			υ	kinematic fluid viscosity (cm^2/s)

1. Introduction

The characterization of the physical and chemical properties of aerosols is a recurrent need in numerous studies and research projects conducted in occupational health, atmospheric chemistry and physics, stack emissions, etc.

This need is particularly felt in studies on the risk associated with nanomaterials (NM), as it is necessary to be able to distinguish particles related to NM from those of the background (urban background, other nearby sources, etc.).

Transmission electronic microscopy (TEM) coupled with the analysis by Energy Dispersive X-ray (EDX) is part of the techniques responding to this need for characterisation as it allows the physical, chemical, morphological and individual analysis of the particles deposited on a support adapted to it, to be specific, a TEM grid. This is the reason that many studies have been conducted for many years to enable the effective deposit of particles directly on this specific support so as to eliminate an additional sample preparation procedure. It is important to emphasise the fact that, at this stage, it is a qualitative, not a quantitative approach.

The TEM grids available on the market are round metallic grids (copper, nickel, gold or molybdenum), approx. 3 mm in diameter, divided into several hundred squares (Figure 1). They are generally provided with a fine, translucent electron beam membrane a few nanometres thick (often a carbon membrane) which allows the contrast of particles deposited on their surface to be viewed. These grids exist on the market under many categories and net size, according to their applications (*Agar scientific*®).

The sampling techniques utilizing TEM grids available today are various. Some are based on the phenomenon of diffusion (Tsai et al. (2009), Cena et al. (2011)), thermophoresis (Lyyränen et al. (2009)), electrostatic precipitation (Dikens & Fissan (1999), Fierz et al. (2007), Li et al. (2010), Miller et al. (2010)), etc.

The sampling technique with TEM grids proposed by Lyyränen et al. (2009) called APS-EM (ASPiration EM grid sampler), consisting of using a porous membrane TEM grid (see Figure 1) to sample particles by filtration is also noted.

Following feasibility studies conducted in a laboratory, this last technique has been applied by R'mili et al. (2011) during a characterisation study of particles emitted during manipulation of

carbon nano-tubes (CNT) powders. It was also applied by Fleury et al. (2011) during a characterisation study of a work environment around an extruder manufacturing composite granules (polymer-CNT), and by Bouillard et al. (2010) to characterize exhaust from a combustion system. These studies have shown that the filtration technique with porous TEM grids allows the sampling of various types of particles (varied in size, shape, etc.), both in the laboratory and in the field. From a practical perspective, the technique has turned out to be easy to use, economical and portable; samples validated for microscopy analysis may be produced with collection times ranging from a few minutes to 30 minutes, depending on application. It is important to note that this technique has turned out to be easier to use than a sampling system by electrostatic precipitation which is more cumbersome and requires prior electrical charge of particles.

As these tests in realistic conditions are convincing it has seemed necessary to accurately evaluate the collection efficiency of this technique is --especially as regards the diameter of the particles--, and to identify the mechanisms of filtration. Moreover, it has seemed important to develop a TEM grid holder that is as versatile as possible and particularly one that connects easily to sampling lines and size selection systems (e.g. pre-impactors, differential mobility analysers (DMA)).

The study presented here covers the evaluation of the collection efficiency of the two main grids available on the market, adapted to the filtration sampling technique through porous TEM grids. It implements a versatile TEM grid holder developed specifically for this application, the MPS® ("Mini-Particle Sampler"®).

2. Materials and method

2.1. TEM porous grids

Three types of porous membrane TEM grids are available on the market: "Lacey", "Holey", and "Quantifoil", each with a different carbon structure. The Lacey type has very large holes (a few micrometres in diameter), the "Holey" type has smaller holes, and the "Quantifoil" type has holes generally calibrated in diameter, evenly spaced and uniformly distributed.

For this study, we have selected a "Holey" type grid (Figure 1-b) and a "Quantifoil" type grid (Figure 1-c), both fitted with a 400 "mesh" grid (Figure 1-a). These grids are available on the market with the following references:

- "Holey" type TEM grid (ref. Cu Holey carbon film 400 mesh, *Agar Scientific*®)
- "Quantifoil" type TEM grid ((ref. Cu Quantifoil 1.2/1.3 400 mesh, *Agar Scientific*®)). In this reference, 1.2 represents the hole diameter in micrometres, and 1.3 the distance between holes.

These two TEM grids have been selected for two main reasons. On the one side, their hole diameter, the smallest of all porous carbon membrane TEM grids which can be found on the market, promotes effective sampling. On the other, their grid (400 mesh) which is the most important. Indeed, on a weaker grid, the carbon membrane will present a more important surface to the air flow and thus risk to yield under the pressure induced by this flow during sampling.

2.2. MPS® sampling system

Called MPS® (Mini-Particle Sampler®), the sampling system developed in this study appears as a TEM grid holder measuring 12 cm x 1.5 cm. It is comprised of two connectors, a male and a female (Figure 2). A TEM grid and a copper joint (the copper joint ensures good air tightness - ref.: Hole Grid Cu 2000µm, *Agar Scientific, external diameter = 3.05 mm, internal diameter = 2 mm*) are respectively placed on the male connector on a support adapted to their size. The female connector is designed to be attached to the male connector and also to keep the TEM grid and joint on their support. By aspiration, the air flow goes through the female connector and the porous TEM grid used via the holes of its membrane and leaves the system via the male connector.

Unlike the device used by Lyyränen et al. (2009), the MPS® is fitted with a tube upstream of the TEM grid, which allows the connection with an equipment (instrument, reactor, etc.). This particular feature, on the other hand, has made it easier to evaluate the collection efficiency of the porous TEM grid used in his study, as the device could be connected directly to a mono-dispersed aerosol source (see section 2.4).

2.3. Method

The capacity of a filter or membrane to collect particles is characterized by the collection efficiency *E*, determined by (Hinds (1999)):

$$E = 1 - P_t \quad (1)$$

with, P_t the penetration (also called penetrating fraction) represents the fraction of particles that goes through the filter medium and is given by:

$$P_t = \frac{N_{Dw}}{N_{Up}} \quad (2)$$

where, N_{Up} and N_{Dw} represent respectively the concentration in number of particles upstream and downstream of the filtering medium.

The determination of the working method was based on the works of Heim et al. (2005). These works take into account several methods of assessing the efficacy of a filtering medium, available in the literature.

In certain approaches, the upstream and downstream filter concentration is measured by two different particle counters, which requires the use of a correction factor to take into account the counters' own intrinsic differences. Certain approaches avoid this constraint by using a single counter.

It is also interesting to set aside the losses by deposition due to the filter holder, in order to focus on the losses due to the filtering medium only. This may be done for example by setting up two devices in parallel: one fitted with filtering medium, the other one not.

From these observations, the method carried out for this study has been based on a single counter and has been focused on the TEM grid efficiency

The selected method is based on the use of a monodisperse aerosol, neutralised, stable over time for the duration of approximately 15 minutes. To ensure counting, a single counter is placed downstream of the filter holder, namely the MPS®. The test comprises of three stages: the second stage fitted with a filtering medium whereas the first and the third ones are not.

Each step lasts approximately 2.5 minutes and produces a result in the form of a total number concentration. These steps are separated by a pause of approximately 2 minutes, required for the removal and installation of the TEM grid.

The validation of the data is based on an aerosol stability criterion which rests on a maximum concentration difference of 5% between the results of the first and last step.

The tests have been conducted for a 0.3 $l.min^{-1}$ flow rate within the MPS®. This value is recommended by Lyyränen et al. (2009) in order to avoid the deterioration of the cabon

membrane of the TEM grid studied. This value was also selected based upon previous experiments (e.g. R'mili (2011), Bouillard (2010), Fleury (2011)); this flow rate requires collection times of a few minutes and is compatible with different applications (measurement in the workplace, in room air, etc.) and microscopy needs (non agglomeration of particles on the sampling surface).

Collection efficiency is calculated on the basis of the ratio of the concentration with (N_{stage2}) and without (N_{stage1}) the TEM grid. Thus Eq. (2) becomes:

$$P_t = \frac{N_{stage\,2}}{N_{stage\,1}} \tag{3}$$

This process has been repeated three times for each diameter and composition of particles in order to have an average efficiency and a standard deviation (cf. Table 2).

2.4. Experimental set-up

The experimental set-up is shown in Figure 3.

An atomiser (TSI, model 3076) followed by a dryer has been used to generate polydisperse sodium chloride (NaCl) aerosol from solutions of NaCl concentration of approximately 0.01 g/l. This configuration has allowed the creation in a stable manner over time of a NaCl aerosol in a range of sizes between approximately 15 and 200 nm.

The range of sizes between approximately 5 nm and 15 nm has been considered thanks to a copper aerosol produced by a spark type generator (Schwyn (1988) - GFG-1000 palas®), technique which has been demonstrated (Roth (2004), Evans (2003)) that it can generate metallic aerosols in a stable manner with an average diameter of approximately 10 to 30 nm.

For both sources, a platform (TSI, model 3080), fitted with a Nano-DMA column (TSI, model 3085) was used for size selection. By using this platform, NaCl aerosol particles were monodispersed between 15 and 150 nm and copper aerosol particles between 5 and 20 nm.

The monodisperse aerosol thus produced has been neutralised by a radioactive source (Krypton 85).

Measurement of the number concentration at the outlet of the MPS® collector was determined using a CNC (TSI, model 3775).

3. Theory

The TEM grids selected in this study are comparable to a microporous membrane. Given their geometric characteristics, the "capillary tube model" was chosen (Rubow et Liu, 1986), an approach started by J. Pich (1964). This model consists in assimilating the structure of a microporous membrane to a group of capillary holes, with the same section, uniformly distributed, equally distant, and perpendicular to its surface in a way as to consider the system (flow of carrier fluid and behaviour of particles) starting from a unitary hole.

The collection efficiency by filtration of a membrane depends on many physical mechanisms. In the absence of any external field of energy other than gravity, the most important ones are inertial impaction, interception and Brownian diffusion ((K. L. Rubow & B. Y. H. Liu (1986)). The existing theoretical models are generally formulated starting from the expressions of efficiency of each of these mechanisms supposed to act independently from each other.

It is essential to take into account the potential role of the thickness of the filtering media: Cyrs et al. (2010) have noted the predominant character of this parameter for membranes which are only 10 µm thick. In the case of the selected TEM grids, the carbon membrane is of a particularly low thickness (L< 20 nm). This allows the hypothesis that the deposit of particles in the internal walls of the holes is negligible, indeed, non-existent. In this case, it's solely a surface deposit. As a result, our theoretical approach consists in considering only expressions of the fraction of surface deposit, that is, by impaction, by interception and by surface diffusion.

As for the capillary tube model, the microporous carbon membrane of a TEM grid may be characterised by a characteristic hole diameter D_0 a surface hole density N_0 (number of holes per surface unit) and a porosity P. The latter parameter represents the fraction of the total membrane surface occupied by the opening of the holes. It may be given by the following equation (adapted from Manton (1978, 1979):

$$P = A_0 N_0 = \pi R_0^2 N_0 \qquad (4)$$

where, A_0 is the area occupied by the opening of a beam hole R_0.

The unitary hole (Figure 4) may be considered as a ring of the internal beam R_0 and of the external beam R_e. The latter is given by the following equation (adapted from Manton (1978, 1979):

$$R_e = \frac{R_0}{\sqrt{P}} \tag{5}$$

The flow of carrier fluid may be characterised by the noted frontal velocity U_0. It is the speed at which the carrying fluid approaches the membrane. It depends on the geometry of the filter holder of the flowrate of the sampling Q. As the MPS® is a cylinder tube with a section S, the frontal velocity may be obtained by the following equation:

$$U_0 = \frac{Q}{S} \tag{6}$$

Moreover, the existing theoretical expressions are developed based on an approach according to which the flow of the carrying fluid as it approaches a hole is considered like the flow into the cylinder tube of a beam R_e (Figure 4). As the latter is generally of the order of micrometers, the flow is supposed to be laminar in the Stokes' regime, i.e., with a low Reynolds number (Re < 1). In fact, this allows a simplification of the system studied. Reynolds number is given in this case by the following equation:

$$Re = R_e U_0 / \upsilon \tag{7}$$

where, υ is the kinematic fluid viscosity ($\upsilon \approx 0.15$ cm^2/s for air).

Thus, the collection efficiency (E_{Im}) due to inertial impaction takes on the following expression (Pich (1964)):

$$E_{Im} = \frac{2\epsilon_{im}}{1+\xi} - \left(\frac{\epsilon_{im}}{1+\xi}\right)^2 \tag{8}$$

with,

- E_{Im} the collection efficiency due to the impaction mechanism,

- ξ : a parameter that takes into account membrane porosity and is expressed as:

$$\xi = \frac{\sqrt{P}}{1-\sqrt{P}} \tag{9}$$

- ϵ_{im} an impaction parameter given by:

$$\epsilon_{im} = 2Stk\sqrt{\xi} + 2Stk^2\xi exp\left[-\frac{1}{Stk\sqrt{\xi}}\right] - 2Stk^2\xi \quad (10)$$

- Stokes *Stk* number is expressed:

$$Stk = \frac{\rho_P d_p^2 U_0 C_c}{9\eta D_0} = \frac{mU_0 C_c}{6\pi\eta r_p R_0} \quad (11)$$

The Cunningham correction factor takes into account the discontinuity of the medium and is expressed:

$$C_c = 1 + Kn[a + bexp(-c/Kn)] \quad (12)$$

a, b, c are experimentally determined coefficients. Numerous values are attributed to these coefficients. For this study, we have considered those proposed by Kim et al. (2005): a = 1.165, b = 0.483 and c = 0.997, determined with the help of a nano-DMA.

Kn, Knudsen's number, is a dimensionless number defined as the relationship between the free mean flow of gas molecules carrying λ_g and the physical diameter of the particle d_p , and is expressed:

$$Kn = 2\lambda_g/d_p \quad (13)$$

In the case of the collection efficiency by filtration due to interception (E_{In}), many expressions have been proposed (Spurny et al. (1969), T. N. Smith et al. (1976), Smith and C. R. Phillips (1975), Happel and Berner (1973), W. John and G. Reischl (1978), Marre and Palmeri (2001)) out of which the one proposed by John and G. Reischl (1978) has been considered the most appropriate in case of a porous TEM grid:

$$E_{In} = (2R - R^2)^{\frac{3}{2}} \quad (14)$$

with R a dimensionless interception parameter given by $R = r_p/R_0$

For collection efficiency due to Brownian diffusion, most of these existing models only take into account transfers by particle diffusion toward the internal walls of the holes (Twomey

(1962), Gormley (1949), Marre (2001, 2004)). This assumes that the transfers by particle diffusion toward the membrane surface are negligible. However, Smith et al. (1976) and recently Cyrs et al. (2010) have shown that these transfers may also be very important.

Manton (1979) had already studied the issue and proposed an expression to this effect; yet he did not consider it to be satisfying, putting forth a likely problem at the level of definition of the diffusion parameter. It actually happens that this expression does not agree with the experimental results of this study, as it does not agree with the results obtained by Kirsch & Spurny (1969), Liu & Lee (1976) and Smith et al. (1976),

As a result, it has been necessary to search for different approach. Specifically, this work proposes an adaptation of the model developed by Stechkina and Fuchs (1966), Kirsch and Fuchs (1969) starting from Kuwabara's cell flow model Kuwabara (1959):

$$E_{Ds} = 2{,}9 Ku^{-1/3} Pe_p^{-2/3} \tag{15}$$

where $Ku = -\ln(\alpha/2) - \frac{3}{4} + \alpha - \frac{\alpha^2}{4}$ $(\alpha = 1 - P)$, represents the solid fraction of the membrane,

In fact, in our case $Pe_p = \frac{D_0 U_0}{D}$ represents Péclet's number related to the characteristic hole diameter D_0 of the membrane.

In the absence of interactions of streamline flows in the inter-pore space, the total fraction of the penetrating particles is equal to the product of penetration efficiency attributed to each mechanism. Therefore, the total collection efficiency can be expressed as (Hinds 1999):

$$E = 1 - \Pi P_t = 1 - (1 - E_{Im})(1 - E_{In})(1 - E_D) \tag{16}$$

4. Characteristics of grids and flow

To use the above models, the following is required:

1. To characterise the structure of the TEM grids examined by determining the following parameters: the characteristic hole diameter of membrane $D_{0,}$ the surface density of

holes N_0 (number of holes per surface unit) and membrane porosity P. These parameters are required for the calculations.

2. Verify that the flow of carrying fluid when it approaches a hole is laminar, in the Stokes' regime, in which case the above expressions are valid.

4.1. Characteristics of TEM grids examined

The characteristics of the TEM grids selected have been determined experimentally by processing images taken by TEM with the help of a library of algorithms integrated to an image processing software (Visilog®).

Table 1 collects the characteristics recorded on a dozen grids, for each of the two types of TEM grids studied.

One may notice that the characteristic parameters of "Quantifoil 1.2/1.3" TEM grids do not change between grids. The same does not apply to "Holey" TEM grids, whose characteristic parameters may differ between grids and sometimes significantly.

4.2. Nature of carrier fluid flow

On the one side, the TEM grid is placed within a cylinder measuring 2 mm in diameter (Figure 2). On the other, the flowrate selected for this study is 0.3 l/min (see 2.3). This parametering makes the mean fluid velocity in this conduit rise to 1.6 m/s (Equation 6). This velocity is considered in our case as the frontal velocity of the carrying fluid U_0 (see. Section 3).

In the capillary tube model, the carrying fluid flow when it approaches a hole of the membrane is considered as being a flow into a cylinder beam tube R_e (equation 5). Its nature is given by the Reynolds number (equation 7). In our case and according to the characteristics of the TEM grids studied, the values obtained are presented in Table 1.

As *Re* is <1, the flow is therefore laminar, in the Stokes' regime. The above models would therefore be valid in our conditions (sampling flowrate, geometry of sampling systems and characteristics of the two TEM grids studied).

5. Results

Figures 5 and 6 present the collection efficiency of TEM grids "Quantifoil 1.2/1.3" and "Holey", respectively, data also available in Table 2. In both cases, the values presented are an average of results of at least three tests.

A theoretical estimate is also presented for both cases of grids. In the case of "Holey" grids, three theoretical curves are proposed according to hole diameter: the high curve and the low curve corresponding to the extreme diameter values (high and low respectively) shown in Table 1; the central simulation (solid line) corresponds to the average diameter.

For both types of grid, a very good theory-experiment convergence is observed, on the entire 5 nm – 150 nm range. A minimum collection efficiency is obtained for particles with a diameter between 20 and 40 nm (diameter of electrical mobility).

This minimum efficiency is evaluated at approximately 15% for "Quantifoil 1.2/1.3" type grids and approximately 18% for "Holey" type grids. This diameter range corresponds, in our conditions (sampling speed equal to 1.6 m/s and characteristics of TEM grids studied), to the particles least sensitive to the different collection mechanisms.

The collection efficiency of both TEM grids is all the more important as the diameter of the particles reaches the area 20 – 40 nm, simultaneously toward the higher or lower diameters.

In the case of "Quantifoil 1.2/1.3", the relative standard deviation of the experiment remains lower than or equal to 10%, which shows a very good reproducibility of the collection system (Table 2).

In the case of "Holey" grids (Table 2), the relative standard deviation of the experiment is less satisfying, between 5 and 15%. This would be due to the main difference existing between both types of grid, in particular the shape and diameter of the holes. Indeed, if the "Quantifoil" type has holes of constant shape and size (see. Figure 1-c), this is not the case for the "Holey" type, which shows a significant variation of the shape (see. Figure 1-b) and size of its holes (see. Table 1). Figure 6 shows the simulations obtained for the extreme values of the diameter: the difference between them in absolute values varies from 10% toward 30 nm, up to 30% at 150 nm.

Whatever the grid, the total collection efficiency turns out to be more important than by electrostatic precipitator, which, not mathematically corrected, is lower than 1% (Li et al.

(2010), Bau et al. (2010), Le Bihan et al. (2011)). Indeed, in this system, the surface of the TEM grid represents only a very minor part of the totality of particles collected on the surface deposition (electrode).

6. Behaviour of particles

This part lies only on the "Quantifoil 1.2/1.3" TEM grid, on account of its well defined structure (shape and size of holes) and reduced standard deviation (< 10%) obtained in the experimental section of the study.

Figure 7 shows experimental results as well as a theoretical estimate obtained for the collection efficiency with a "Quantifoil 1.2/1.3" TEM grid. The theoretical estimate distinguishes the impact of different collection mechanisms, i.e., inertial impaction, interception and diffusion.

The simulation shows that impaction and diffusion are the prevailing mechanisms, with impaction dominating the collection of particles above 30 nm, and diffusion dominating the collection of particles under 30 nm. The contribution of the interception mechanism to the collection only becomes significant for the particles whose diameter is above 200 nm.

This interpretation seems to be confirmed by observations of the grids studied by TEM (Figure 8) for which, it may be noted that most of the particles collected seems to be deposited on the surface of the membrane.

Moreover, it should be noted that the general appearance and dimensions of collection efficiency observed here show strong similarities with the experimental results obtained by Cyrs et al. (2010) for the surface collection efficiency, despite a relatively different membrane porosity and frontal velocity.

.

7. Conclusion and perspectives

Filtration on porous TEM grid is a new particle sampling technique in view of an analysis by transmission electron microscopy.

A TEM grid holder has been especially developed to allow the implementation of this technique in the simplest, fastest, and most versatile manner possible: it is the MPS® (Mini-Particle Sampler®).

The study described here on the implementation of this filtration technique, with the help of MPS® and both market products most often adapted today, in particular Quantifoil TEM (1.2/1.3) and Holey TEM porous TEM grids.

The collection efficiency of these two grids has been tested experimentally on a generation bed of mono-dispersed copper and sodium chloride aerosol. Tests show that the collection is operational in the 5 nm - 150 nm size range, with a minimum efficiency around 30 nm of 15-18%.

The collection efficiency has also been simulated, by relying on the studies done on porous membrane. The results obtained are consistent with the experimental results and show the prevailing character of the mechanisms of diffusional deposition by diffusion, under 30 nm and of impaction deposition, above 30 nm.

The simulation shows an increased efficiency around the small and large sizes.

This study shows therefore the validity of the filtration concept by porous TEM grid.

This technique is particularly simple when compared with other TEM grid collection techniques. Indeed, in addition to a filter holder and a pump, most of these techniques must implement supplementary and energy consuming tools with the aim of having an active element such as an electric field or a thermal gradient.

The modest size of the filter holder makes it a very good tool for individual collections (R'mili (2011), Fleury (2010)). It could also be easily integrated in experimental devices: measurement downstream of a DMA, collection at reactor outlet (Bouillard (2010)), etc.

The filter holder designed in this study is now commercially available as a low cost, portable and easy to use tool.

8. Acknowledgement

The authors thank the Picardy region and the Ministry for the Environment (programme 190) for their financial support.

They also thank Laurence Le Coq, Aurélien Zantman, Emmanuel Peyret, Sophie Mary, Neeraj Shandilya, Aurélien Ustache and Christophe Bressot for their support.

References

Bau S., Ouf F. X., Miquel S., Rastoix O. et Witschger O. (2010). Experimental measurement of the collection efficiency of nanoparticle samplers based on electrostatic and thermophoretic precipitation. International Aerosol Conference, Helsinki, Finland.

Cena L. G., Anthony T. R., Peters T. (2011). A Personal Nanoparticle Respiratory Deposition (NRD) Sampler. *Environmental Science and Technology,* 45, 6483-6490.

Cheng Y. S. et Yeh H. C. (1980). Theory of a screen-type diffusion battery. *Journal of Aerosol Science*, 11(3), 313-320.

Chengjue Lia, Shusen Liub, Yifang Zhuc, "Determining Ultrafine Particle Collection Efficiency in a Nanometer Aerosol Sampler", *Aerosol Science and Technology*, Volume 44, Issue 11 November 2010 , pages 1027 – 1041.

Cyrs W. D., Boysen D. A., Casuccio G., Lersch T. et Peters T. M. (2010). Nanoparticle collection efficiency of capillary pore membrane filters. *Journal of Aerosol Science*, 41(7), 655-664.

Dixkens J. et Fissan H. (1999). Development of an electrostatic precipitator for off-line particle pnalysis. *Aerosol Science and Technology*, 30(5), 438-453.

Evans D. E., Harrison R. M. et Ayres J. G. (2003). The generation and characterization of metallic and mixed element aerosols for human challenge studies. Aerosol Science and Technology, 37(12), 975-987.

Fierz M., Kaegi R. et Burtscher H. (2007). Theoretical and experimental evaluation of a portable electrostatic TEM sampler. *Aerosol Science and Technology*, 41(5), 520-528.

Fleury D., Bomfim J. A. S., Vignes A., Girard C., Metz S., Munoz F., R'Mili B., Ustache A., Guiot A. et Bouillard J. X. (2011). Identification of the main exposure scenarios in the production of CNT-polymer nanocomposites by melt-moulding process. *Journal of Cleaner Production* (0).

Gormley P. G. et Kennedy M. (1949). Diffusion from a stream flowing through a cylindrical tube. Proc. Roy. Irish Academy, Vol 52A, 163-169.

Happel J. et Bernner H. (1973). Low Reynolds number hydrodynamics. *Noordhoff International, Leyden*, 150-153.

Heim M., Mullins B. J., Wild M., Meyer J. et Kasper G. (2005). Filtration efficiency of aerosol particles below 20 nanometers. *Aerosol Science and Technology,* 39(8), 782-789.

Hinds W. C. (1999). *Aerosol Technology – Properties, Behaviour and measurement of Airborne Particles*. Second edition, John Wiley & Sons, New York, p. 203.

John W., Reischl G., Goren S. et Plotkin D. (1978). Anomalous filtration of solid particles by Nuclepore filters. *Atmospheric Environment*, 12(6-7), 1555-1557.

Kim J. H., Mulholland G. W., Kukuck S. R. et Pui D. Y. H. (2005). Slip correction measurements of certified PSL nanoparticles using a nanometer differential mobility

analyzer (Nano-DMA) for knudsen number from 0.5 to 83. *Journal of Research of the National Institute of Standards and Technology*, Vol. 110, 31-54.

Kirsch A. A. et Fuchs N. A. (1968). Studies on fibrous aerosol filters - III Diffusional deposition of aerosols in fibrous filters. *The Annals of Occupational Hygiene*, 11(4), 299-304.

Kirsch A. A. et Spurny K. R. (1969). Gas flow in Nuclepore filters. Journal of app. mech. tech. phys., 10 109-112.

Le Bihan O., Zantman A., Thévenet S., R'mili B. et Ustache A. (2011). *Assessment of the sampling efficiency of an electrostatic precipitator.* Congrès Français sur les Aérosols, Actes de Congrès, 6 pages, 2011, Paris.

Li C. J., Liu S. S. et Zhu Y. F. (2010). Determining ultrafine particle collection efficiency in a nanometer aerosol sampler. *Aerosol Science and Technology*, 44(11), 1027-1041.

Liu B. Y. H. et Lee K. W. (1976). Efficiency of membrane and nuclepore filters for submicrometer aerosols. Environmental Science & Technology, 10(4), 345-350.

Lyyränen J., Backman U., Tapper U., Auvinen A. et Jokiniemi J. (2009). A size selective nanoparticle collection device based on diffusion and thermophoresis. *Journal of Physics: Conference Series*, 170.

Manton M. J. (1978). The impaction of aerosols on a nucleopore filter. Atmospheric Environment, 12 1669-1675.

Manton M. J. (1979). Brownian diffusion of aerosols to the face of a nuclepore filter. Atmospheric Environment, 13(4), 525-531.

Marre S. et Palmeri J. (2001). Theoretical study of aerosol filtration by nucleopore filters: the intermediate crossover regime of brownian diffusion and direct interception. Journal of Colloid and Interface Science, 237(2), 230-238.

Marre S., Palmeri J., Larbot A. et Bertrand M. (2004). Modeling of submicrometer aerosol penetration through sintered granular membrane filters. Journal of Colloid and Interface Science, 274(1), 167-182.

Miller A., Frey G., King G. et Sunderman C. (2010). A handheld electrostatic precipitator for sampling airborne particles and nanoparticles. *Aerosol Science and Technology*, 44(6), 417-427.

Pitch J. (1964). Impaction of aerosol particles in the neighbourhood of a circular hole. *Collection Czechoslovak of Chemical Communications*, 29 2223-2227.

R'mili B., Dutouquet C., Sirven J., Aguerre-Chariol O. et Frejafon E. (2011). Analysis of particle release using LIBS (laser-induced breakdown spectroscopy) and TEM (transmission electron microscopy) samplers when handling CNT (carbon nanotube) powders. *Journal of Nanoparticle Research*, 13(2), 563-577.

Roth C., Ferron G. A., Karg E., Lentner B., Schumann G., Takenaka S. et Heyder J. (2004). Generation of ultrafine particles by spark discharging. Aerosol Science and Technology, 38(3), 228-235.

Rubow K. L. et Liu B. Y. H. (1986). Characteristics of membrane filters for particle collection in fluid filtration, Gas, vol. 1, ASTM Tech. Pub. 975, Philadelphia, PA.

Schwyn S., Garwin E. et Schmidt-Ott A. (1988). Aerosol generation by spark discharge. *Journal of Aerosol Science*, 19(5), 639-642.

Smith T. N. et Phillips C. R. (1975). Inertial collection of aerosol particles at circular aperture. *Environmental Science & Technology*, 9(6), 564-568.

Smith T. N., Phillips C. R. et Melo O. T. (1976). Diffusive collection of aerosol particles on Nuclepore membrane filter. *Environmental Science & Technology*, 10(3), 274-277.

Spurny K., Lodge J. P., Frank E. R. et Sheesley D. C. (1969). Aerosol filtration by means of Nuclepore filters: structural and filtration properties. *Environmental Science & Technology*, 3(5), 453-464.

Stechkina I. B. et Fuchs N. A. (1966). Studies on fibrous aerosol filters - I. Calculation of diffusional deposition of aerosols in fibrous filters. *The Annals of Occupational Hygiene*, 9(2), 59-64.

Twomey S. (1962). Equations for the decay of diffusion of particles in an aerosol flowing through circular and rectangular channels. Bull. Obs. Puy de Dome, Vol 10, 173-180.

Tsai S.-J., Ada E., Isaacs J. et Ellenbecker M. (2009). Airborne nanoparticle exposures associated with the manual handling of nanoalumina and nanosilver in fume hoods. *Journal of Nanoparticle Research*, 11(1), 147-161.

Figure 1: examples of TEM porous grids – case of a “Holey” type and ‘Quantifoil’ type

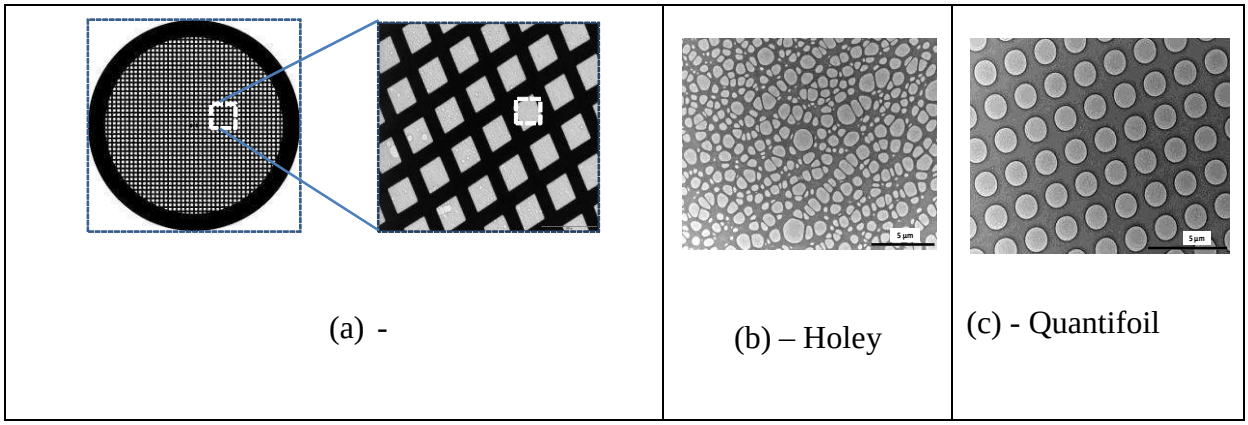

(a) -

(b) – Holey

(c) - Quantifoil

Figure 2: concept diagram of the filter holder

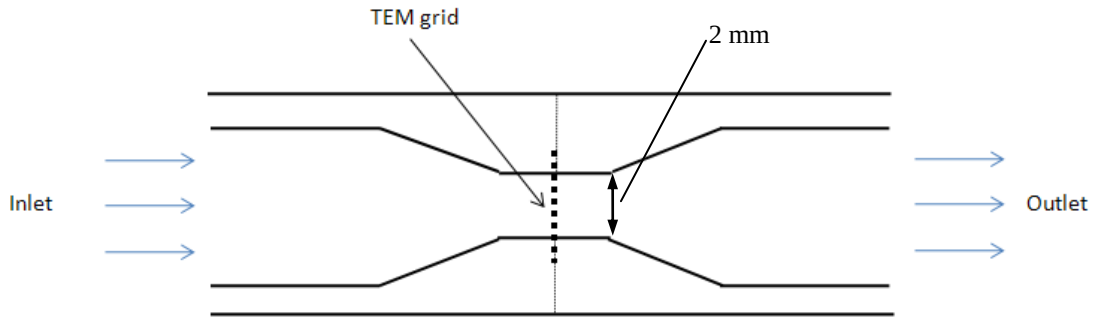

Figure 3: Concept diagram of the experimental set-up

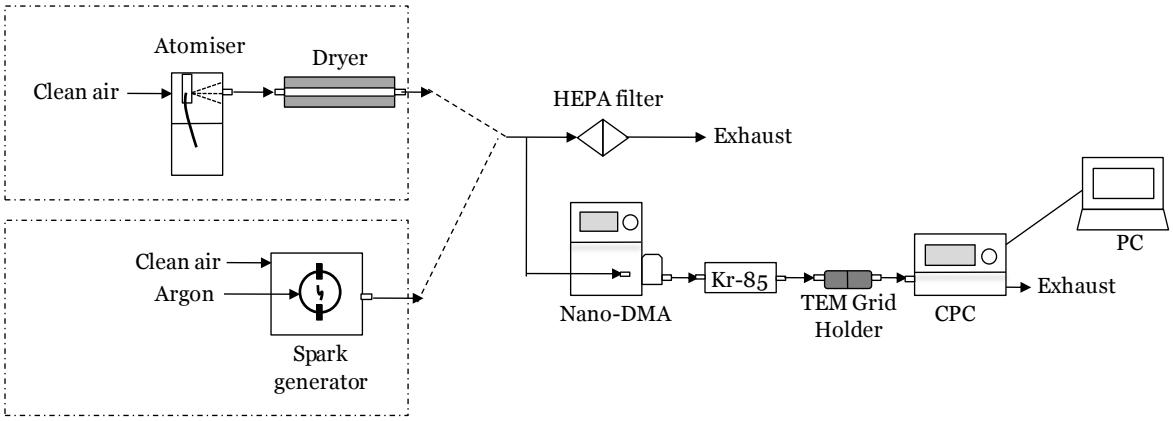
Atomiser
Dryer
Clean air
HEPA filter
Exhaust
Clean air
Argon
Spark
generator
Nano-DMA
Kr-85
TEM Grid
Holder
CPC
Exhaust
PC

Figure 4: characteristics of a unitary hole

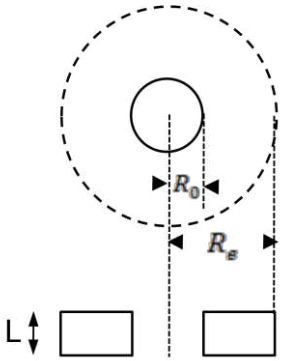

Figure 5: Particle collection efficiency by size for the Quantifoil 1.2/1.3 TEM grid. The theoretical collection efficiency has been calculated using the parameters related to the operation conditions and characteristics of the TEM grid (cf. Table 1).

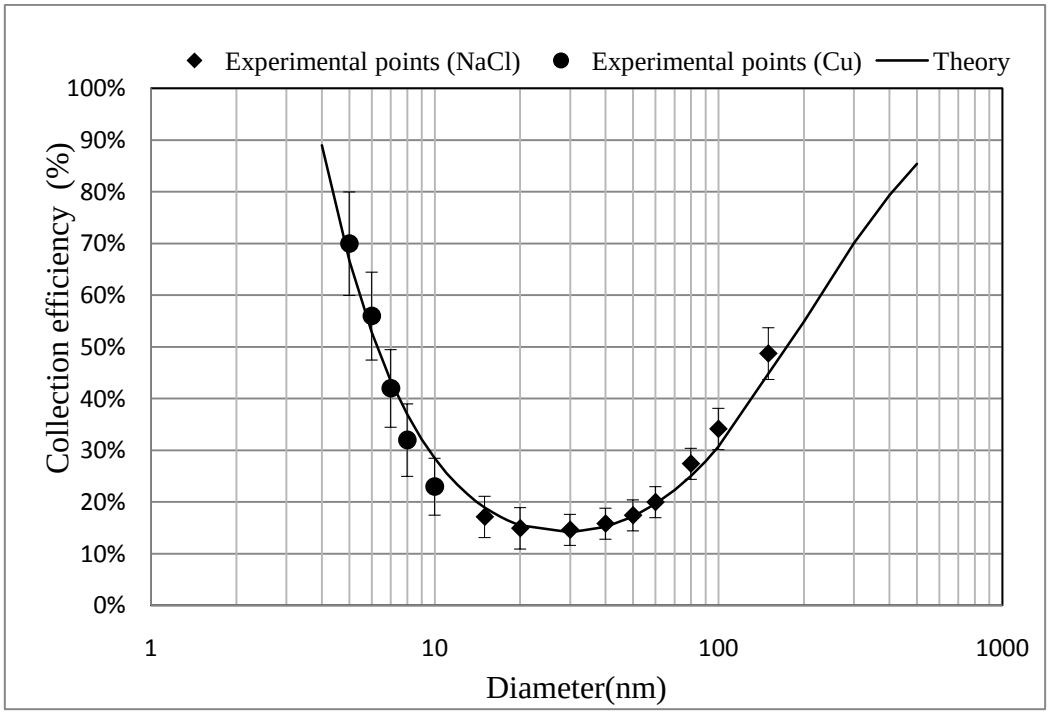

Figure 6: Particle collection efficiency by size for the Holey TEM grid. The theoretical collection efficiency has been calculated using the parameters related to the operation conditions and characteristics of the TEM grid (cf. Table 1).

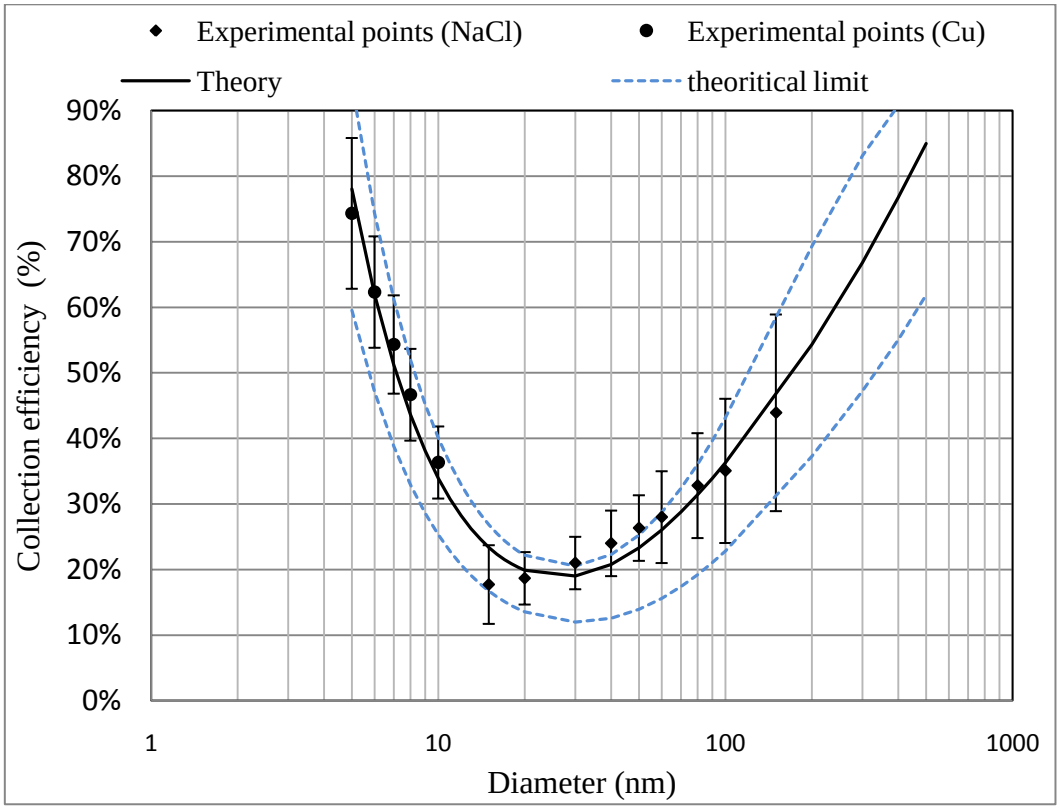

Figure 7: Comparison of experimental and theoretical approaches to assessing collection efficiency of the Quantifoil 1.2/1.3 TEM grid.

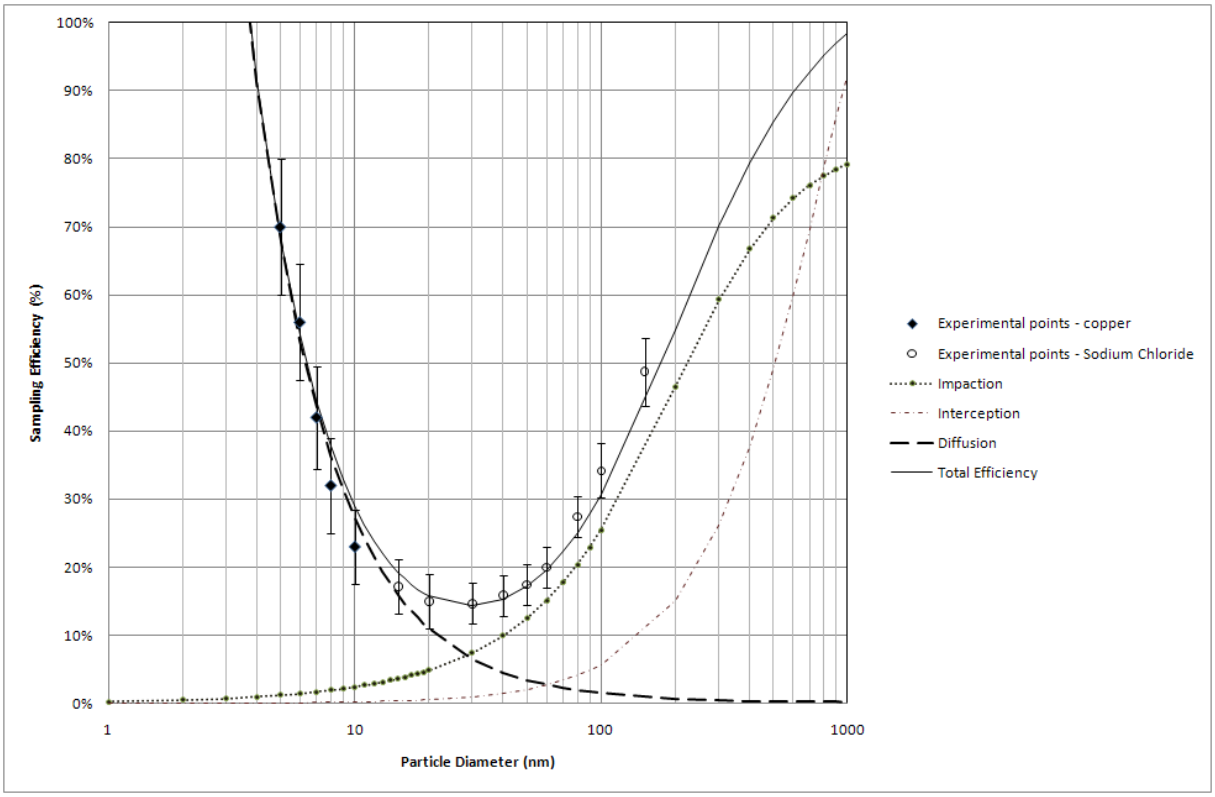

Figure 8: Examples TEM images of NaCl and Cu collected particles from a polydisperse aerosol.

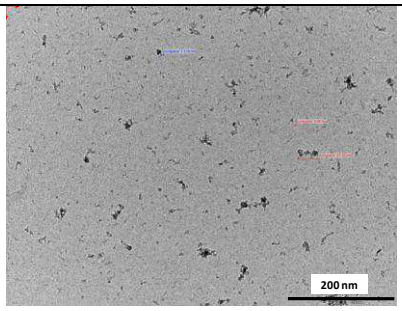

Cu.

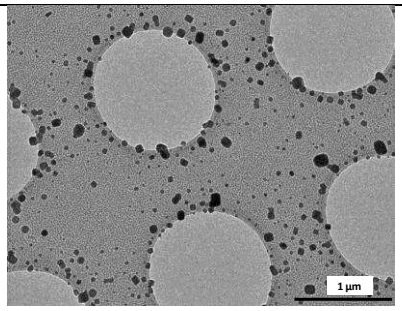

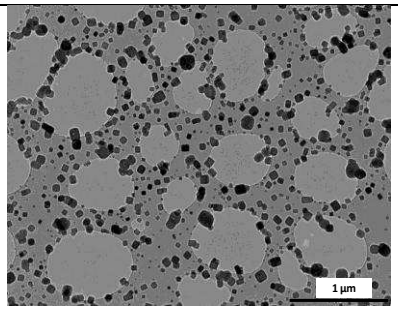

NaCl

Cu – polydispersed

NaCl - polydispersed

Table 1: Structural characteristics of the Quantifoil 1.2/1.3TEM grid 400 mesh carbon membrane and of the Holey membrane. The characteristic parameters of "Holey" TEM grids are given indicatively, as they concern only the grids used in this study. The Reynolds number is calculated according to the characteristics of the two TEM grids studied for a sampling speed U_0 = 1.6 m/s.

Characteristic parameters	Holey	Quantifoil 1.2/1.3
Pore diameter D_0 (µm)	0.8 – 1.6*	1.3**
Density of pores N_0 (# /cm^2)	2,9.10^7 – 1,1.10^8	1,3.10^7
Porosity P (%)	40 - 65	17
Re (Equation 7)	0.05 – 0.11	0.16

*domain of recorded average hole diameters. The actual recorded hole diameters are between approximately 0.15 and 5 µm

**according to supplier D_0 = 1.2 µm and for measurements for TEM D_0 = 1.3 µm is found

Table 2: Measured overall collection efficiencies for each mean diameter of mono-disperse aerosol and each porous grid.

Particle diameter (nm)		Holey		Quantifoil	
		Overall collection efficiency (%)	Standard deviation (%)	Overall collection efficiency (%)	Standard deviation (%)
5	Cu	74	12	70	10
6	Cu	62	9	56	9
7	Cu	54	8	42	8
8	Cu	47	7	32	7
10	Cu	36	6	23	6
20	Cu	19	8	16	8
15	NaCl	18	6	17	4
20	NaCl	19	4	15	4
30	NaCl	21	4	15	3
40	NaCl	24	5	16	3
50	NaCl	26	5	17	3
60	NaCl	28	7	20	3
80	NaCl	33	8	27	3
100	NaCl	35	11	34	4
150	NaCl	44	15	49	5